

Cosmological 21cm experiments: Searching for a needle in a haystack

Vibor Jelić* †

ASTRON, P.O. Box 2, 7990 AA Dwingeloo, the Netherlands

E-mail: jelic@astron.nl

There are several planned and ongoing experiments designed to explore the Epoch of Reionization (EoR), the pivotal period during which the gas in the intergalactic medium went from being entirely neutral to almost entirely ionized. These experiments will probe the EoR, through the redshifted 21 cm line from neutral hydrogen, using radio arrays: e.g. Low Frequency Array (LOFAR) and Murchinson Widefield Array (MWA). Unfortunately however, the cosmological 21 cm signal is highly contaminated by astrophysical foregrounds and by non-astrophysical and instrumental effects. Therefore, to reliably detect the cosmological signal, it is essential to understand very well all data components, their influence on the desired signal and explore additional complementary or corroborating probes of the EoR. These proceedings give an overview of observational constrains of the foregrounds, present theoretical efforts to model the foregrounds, and discuss a problem of the foreground removal. The major results are presented for the LOFAR-EoR experiment.

ISKAF2010 Science Meeting - ISKAF2010

June 10-14, 2010

Assen, the Netherlands

*Speaker.

†on behalf of the LOFAR-EoR team

1. Introduction

About four hundred million years after the Big Bang the first objects were formed, which then started to ionize the surrounding gas with their strong radiation. Six hundred million years later, the all-pervasive gas was transformed from a neutral to an ionized state. This pivotal period in the history of the Universe is called the Epoch of Reionization (EoR). It holds the key to structure formation and evolution, but also represents a missing piece of the puzzle in our current knowledge of the Universe.

Currently, this is changing through several planned and ongoing experiments designed to probe the Epoch of Reionization (EoR) by detecting redshifted 21 cm emission line from neutral hydrogen: GMRT¹, LOFAR², MWA³, 21CMA⁴, PAPER⁵, and SKA⁶. However, all of these experiments are challenged by strong astrophysical foreground contamination, ionospheric distortions, complex instrumental response, and other different types of noise (see Fig. 1).

In the frequency range of the EoR experiments ($\sim 100 - 200$ MHz) the foreground emission of our own Galaxy and extragalactic sources (radio galaxies and clusters) dominate the sky. In fact, the amplitude of this foreground emission is 4 – 5 orders of magnitude stronger than the expected cosmological 21 cm signal. However, since the radio telescopes, which are used for the EoR observations, are interferometers, they measure only fluctuations of a signal. The ratio between the foregrounds and the cosmological signal is reduced to 2 – 3 orders of magnitude.

In terms of physics, the foreground emission originates mostly from the interaction between relativistic charged particles and a magnetic field, i.e. synchrotron radiation. Galactic synchrotron radiation is the most prominent foreground emission and contributes about 70% to the total emission at 150 MHz [7]. The contribution from the extragalactic synchrotron radiation is $\sim 27\%$, while the smallest contribution ($\sim 1\%$) is from Galactic free-free emission, i.e. thermal radiation of an ionized gas.

Given the prominent foreground emission that needs to be removed from the data in order to reliably detect the EoR signal, cosmological 21 cm experiments can be compared with *finding the needle in the haystack* [1]. However, in the last decade there has been a slew of theoretical and observational efforts to explore and to understand all of the data components of the EoR experiments in order to prepare us for the real data.

These proceedings give an overview of observational constraints of the foregrounds (Sec. 2), present theoretical efforts to model the foregrounds (Sec. 3), and discuss a problem of the foreground removal (Sec. 4). The major results are presented for the LOFAR-EoR experiment, but these results are also applicable to the other EoR projects. The proceedings conclude with future perspective (Sec. 5).

¹Giant Metrewave Telescope, <http://gmrt.ncra.tifr.res.in>

²Low Frequency Array, <http://www.lofar.org>

³Murchinson Widefield Array, <http://www.mwatelescope.org/>

⁴21 Centimeter Array, <http://21cma.bao.ac.cn/>

⁵Precision Array to Probe EoR, <http://astro.berkeley.edu/~dbacker/eor>

⁶Square Kilometer Array, <http://www.skatelescope.org/>

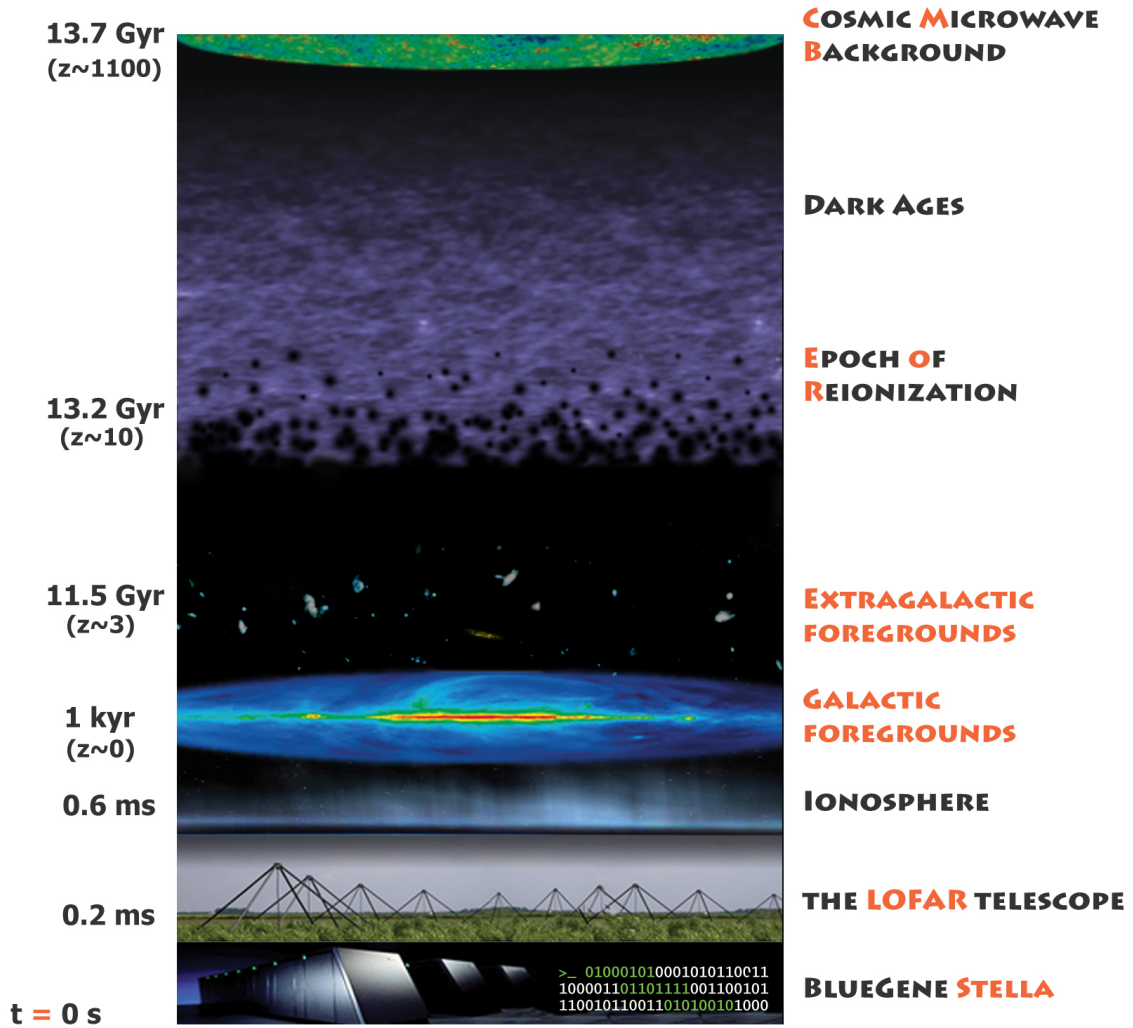


Figure 1: This sketch illustrates all contributions to and contaminations of the observed signal in the case of the LOFAR-EoR key science project [1]. The former are: Galactic ($\sim 71\%$) and extragalactic ($\sim 27\%$) foregrounds [2, 3], CMB $< 1\%$, and the EoR signal $\sim 0.01\%$ [4]; and the latter are: ionosphere, radio frequency interferences [5], and instrumental effects and noise [6]. On the left, a travel time of the observed signal is noted.

2. Observational constrains

There are several all-sky maps of the total Galactic diffuse radio emission at different frequencies and angular resolutions. The 150 MHz map by [8] is the only all-sky map in the frequency range (100 – 200 MHz) relevant for the EoR experiments, but has only 5° resolution.

In addition to current all-sky maps, a number of recent dedicated observations have given estimates of Galactic foregrounds in small selected areas. [9] have used 153 MHz observations with GMRT to characterize the visibility correlation function of the foregrounds. [10] have measured the spectral index of the diffuse radio background between 100 and 200 MHz. [11] have set an upper limit to the diffuse polarized Galactic emission; and [12, 13, see Sec. 2.2] obtained the most

recent and comprehensive targeted observations with the Westerbork Synthesis Radio Telescope (WSRT).

The extragalactic foregrounds at the low radio frequencies are constrained by the source counts from 3CRR catalog at 178 MHz [14] and 6C survey at 151 MHz [15]. However, both catalogs are too shallow for the purpose of the EoR experiments.

2.1 Galactic diffuse emission

At high Galactic latitudes the minimum brightness temperature of the Galactic diffuse emission is about 20 K at 325 MHz with variations of the order of 2 per cent on scales from 5 to 30 arcmin across the sky [16]. At the same Galactic latitudes, the temperature spectral index of the Galactic emission is about -2.55 at between 100 and 200 MHz [e.g. 10, and references therein] and steepens towards higher frequencies. Furthermore, the spectral index gradually changes with position on the sky. This change appears to be caused by a variation in the spectral index along the line of sight. An appropriate standard deviation in the power law index, in the frequency range 100–200 MHz appears to be of the order of ~ 0.1 [7].

Using the obtained values at 325 MHz and assuming the frequency power law dependence, the Galactic diffuse emission is expected to be 140 K at 150 MHz, with ~ 3 K fluctuations.

Studies of the Galactic polarized diffuse emission are done mostly at high radio (~ 1 GHz) frequencies. At lower frequencies (~ 350 MHz), there are several fields done with the Westerbork telescope (WSRT). These studies [17, a review] revealed a large number of unusually shaped polarized small-scale structures of the Galactic emission, which have no counterpart in the total intensity. These structures are usually attributed to the Faraday rotation effects along the line of sight.

2.2 LOFAR-EoR team observations with WSRT telescope

Recently, a comprehensive program was initiated by the LOFAR-EoR collaboration to directly measure the properties of the Galactic radio emission in the frequency range relevant for the EoR experiments. The observations were carried out using the Low Frequency Front Ends (LFFE) on the WSRT radio telescope. Three different fields were observed. The first field was a highly polarized region known as the “Fan region” in the 2nd Galactic quadrant at a low Galactic latitude of $\sim 10^\circ$ [12]. The second field was a very cold region in the Galactic halo ($l \sim 170^\circ$) around the bright radio quasar 3C196, and third was a region around the North Celestial Pole [NCP, $l \sim 125^\circ$; 13]. The last two fields represent possible targets for the LOFAR-EoR observations. Below we present the main results of these papers.

In the “Fan region”, fluctuations of the Galactic diffuse emission were detected at 150 MHz for the first time (see Fig. 2). The fluctuations were detected both in total and polarized intensity, with an *rms* of 14 K (13 arcmin resolution) and 7.2 K (4 arcmin resolution) respectively [12]. Their spatial structure appeared to have a power law behavior with a slope of -2.2 ± 0.3 in total intensity and -1.65 ± 0.15 in polarized intensity (see Fig. 2). Note that, due to its strong polarized emission, the “Fan region” is not a representative part of the high Galactic latitude sky.

Fluctuations of the total intensity Galactic diffuse emission in the “3C196” and “NGP” fields were also observed on scales larger than 30 arcmin, with an *rms* of 3.3 K and 5.5 K respectively.

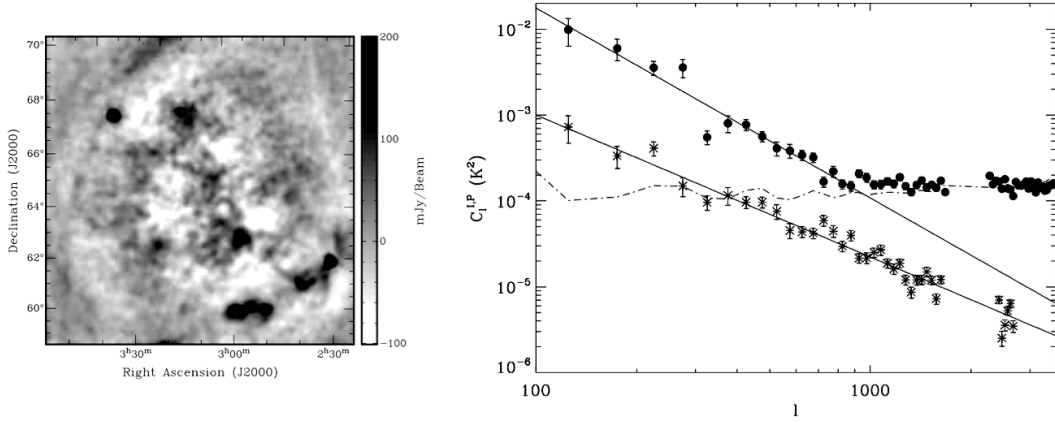


Figure 2: Left panel: Stokes I map of the Galactic emission in Fan region. The conversion factor is $1 \text{ Jy beam}^{-1} = 105.6 \text{ K}$. Right panel: power spectrum (filled circles: total intensity; asterisks: polarized intensity) of the Galactic emission in Fan region with the best power-law fit. [12]

Patchy polarized emission was found in the “3C196” field, with an *rms* value of 0.68 K on scales larger than 30 arcmin [13]. Thus, the Galactic polarized emission fluctuations seem to be smaller than expected by extrapolating from higher frequency observations.

3. Simulations

The foregrounds in the context of the EoR measurements have been studied theoretically by various authors. [7] have given the first overview of the foreground components. [18, 19] have studied emission from unresolved extragalactic sources at low radio frequencies. [20] and [21] have considered the effect of free-free emission from extragalactic haloes. [22] carried out a detailed study of the functional form of the foreground correlations. [2] have made the first detailed foreground model and have simulated the maps that include both the diffuse emission from our Galaxy and extragalactic sources (radio galaxies and clusters). [23] have also studied both galactic and extragalactic foregrounds. [24] have developed a semi-empirical simulation of the extragalactic radio continuum sky that can be used as a extragalactic foreground model. [25] has used all publicly available total power radio surveys to obtain all-sky Galactic maps at the desired frequency range and [26, 27, 28] has developed a detailed Galactic 3D emission simulation that can be used as a Galactic foreground model. [29] has studied foreground contamination in the context of the power spectrum estimation.

3.1 LOFAR-EoR foreground model

Here we give an overview of the foreground model [2, and *submitted*] that is used as a part of the LOFAR-EoR testing pipeline. The model encompasses the Galactic diffuse synchrotron & free-free emission, synchrotron emission from Galactic supernova remnants and extragalactic emission from radio galaxies and clusters. The simulated foreground maps are pertaining in their angular and frequency characteristics to the LOFAR-EoR experiment (see Fig. 3).

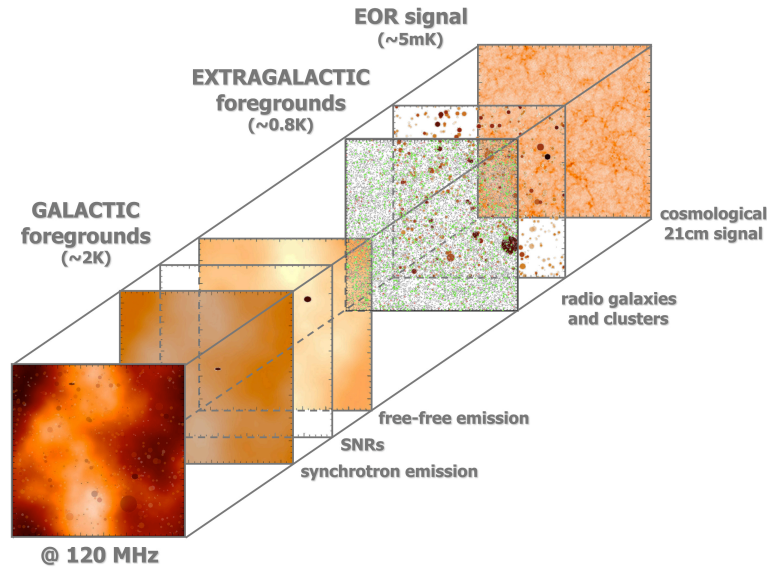


Figure 3: The various simulated Galactic and extragalactic contaminants of the redshifted 21 cm radiation from the EoR. [2]

Since the diffuse Galactic synchrotron emission is the dominant foreground component, all its observed characteristics are included in our model: spatial and frequency variations of brightness temperature and its spectral index, and also the brightness temperature variations along the line-of-sight. Moreover, the Galactic emission is derived from physical quantities and the actual characteristics of our Galaxy (e.g. the cosmic ray and thermal electron density, and the magnetic field). Thus, the model has the flexibility to simulate any peculiar case of the Galactic emission including very complex polarized structures produced by Faraday screens and depolarization.

Despite the minor contribution of the Galactic free-free emission, it is included in our simulations of the foregrounds as an individual component. It has a different temperature spectral index from Galactic synchrotron emission.

Integrated emission from extragalactic sources is decomposed into two components: emission from radio galaxies and from radio clusters. Simulations of radio galaxies are based on the source count functions at low radio frequency by [30], for three different types of radio galaxies, namely FRI, FRII and star forming galaxies. Correlations obtained by radio galaxy surveys are used for their angular distribution. Simulations of radio clusters are based on a cluster catalogue from the Virgo consortium and observed mass–X-ray luminosity and X-ray–radio luminosity relations.

4. Problem of the foreground removal

One of the major challenges of the EoR experiments is the extraction of the EoR signal from the prominent astrophysical foregrounds. The extraction is usually formed in total intensity along frequency, since (see Fig. 4):

1. the cosmological 21 cm signal is essentially unpolarized and fluctuates along frequency;

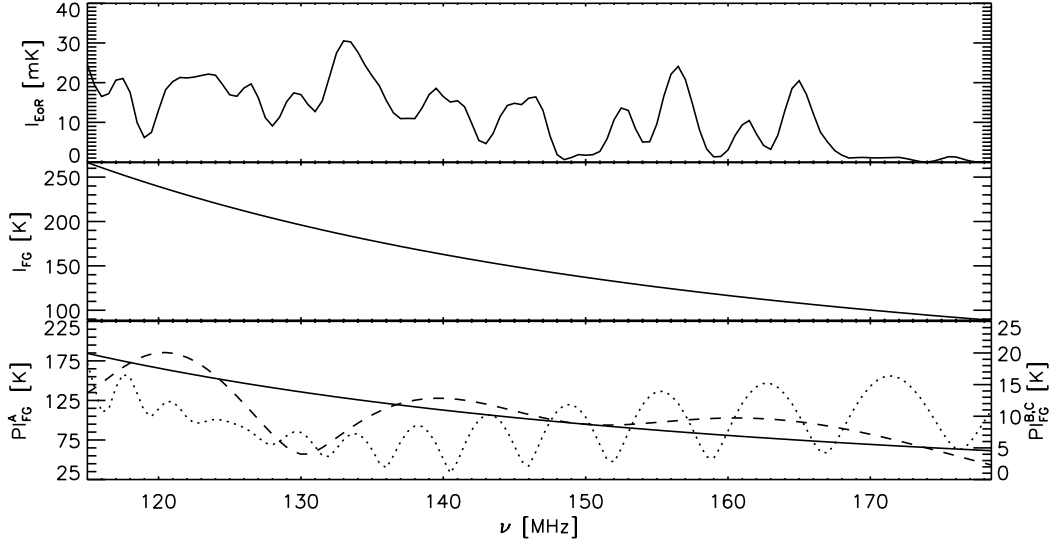


Figure 4: A random line through simulated data cubes (images at different frequencies): cosmological 21cm signal in total intensity (I_{EoR} , [4]), foregrounds in total intensity (I_{FG}), and foregrounds in polarized intensity without (PI_{FG}^A , solid line) and with differential Faraday rotation in the Galaxy (PI_{FG}^{BC} , dashed and dotted line). Note that the foregrounds are smooth along frequency in total intensity and might show fluctuations in polarized intensity. [3]

2. the foregrounds are smooth along frequency in total intensity and might show fluctuations in polarized intensity.

Thus, the EoR signal can be extracted from the foreground emission by fitting out the smooth component of the foregrounds along frequency (see Sec. 4.1). However, all current EoR radio interferometric arrays have an instrumentally polarized response, which needs to be calibrated. If the calibration is imperfect, some part of the polarized signal is transferred into a total intensity and vice versa (hereafter ‘leakage’). As a result, the extraction of the EoR signal is more demanding (see Sec. 4.2).

4.1 LOFAR-EoR experiment: foreground removal methods

The simplest method for foreground removal in total intensity is a polynomial fitting in logarithmic scale. We have showed this using the LOFAR-EoR testing pipeline [2]. However, one should be careful in choosing the order of the polynomial to perform the fitting. If the order of the polynomial is too small, the foregrounds will be under-fitted and the EoR signal could be dominated and corrupted by the fitting residuals, while if the order of the polynomial is too big, the EoR signal could be fitted out. Therefore, we have argued that in principle it would be better to fit the foregrounds non-parametrically (e.g. Wp smoothing) – allowing the data to determine their shape – rather than selecting some functional form in advance and then fitting its parameters [31].

After foreground subtraction from the EoR observations, the residuals will be dominated by instrumental noise, i.e., the level of the noise is expected to be order of magnitudes larger than the EoR signal (assuming 300 h observation with LOFAR). Thus, general statistical properties of the

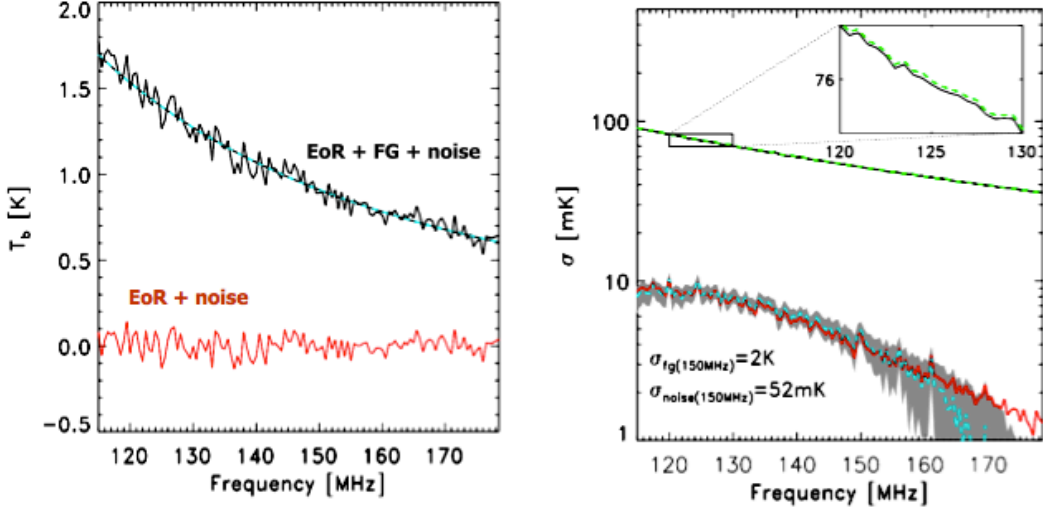


Figure 5: *Left panel:* One pixel along frequency of the simulated LOFAR-EoR data (solid black line), fitted smooth component of the foregrounds (dashed cyan line), and residuals (solid red line) after taking out the foregrounds. Note that the residuals are the sum of the EoR signal and the noise. *Right panel:* Statistical detection of the EoR signal from the simulated LOFAR-EoR data, that include diffuse components of the foregrounds and realistic noise. The dashed-dotted black line represents the standard deviation (σ) of the noise as a function of frequency, the dotted green line the σ of the residuals after taking out the smooth foreground component, and the solid red line the σ of the original EoR signal. The grey shaded zone shows the 2σ detection, whereas the dashed white line shows the mean of the detection. Note that the y-axis is in logarithmic scale. [2]

noise should be determined and be used to statistically detect the cosmological 21 cm signal: e.g., variance of the EoR signal over the image, σ_{EoR}^2 , as a function of frequency (redshift) obtained by subtracting the variance of the noise, σ_{noise}^2 , from that of the residuals, $\sigma_{\text{residuals}}^2$. We have showed such statistical detection of the EoR signal using the fiducial model of the LOFAR-EoR experiment [2] (see Fig.). Note that we have also obtained similar results by using different statistics: the skewness of the one-point distribution of brightness temperature of the EoR signal, measured as a function of observed frequency [32]; and the power spectrum of variations in the intensity of redshifted 21 cm radiation from the EoR [33].

4.2 Problem of the ‘leaked’ polarized foregrounds

In the regions of the Galaxy that have thermal and cosmic-ray electrons mixed, that show significant variations of magnetic field, or both, the polarization angles of Galactic emission are differentially Faraday rotated. If differential Faraday rotation is strong enough, the Galactic polarized emission from that region can behave along frequency in a manner similar to the cosmological 21 cm signal (see Fig. 4). Thus, an inaccurate calibration of instrumental polarized response can transfer a part of such polarized foreground emission in total intensity and mask the desired EoR signal (see Fig. 6).

We have addressed this for the first time through realistic simulations of the LOFAR-EoR experiment [3]. Based on our simulations, we have concluded that the EoR observational windows

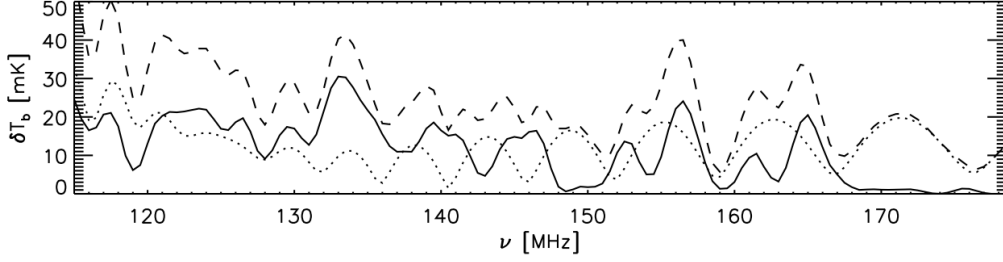


Figure 6: A random line of sight through a simulated 21 cm data cube (solid line). Dotted line shows the ‘leakage’ of the polarized Galactic emission to the total intensity and dashed line is a sum of the two. We assume 0.15% residual ‘leakage’ and we use PI_{FG}^C (see Fig. 4) as an example of the Galactic emission. The angular and frequency resolution of the data match that of the LOFAR telescope. [3]

need to be in the regions with a very low polarized foreground emission, in order to minimize ‘leaked’ foregrounds. Faraday rotation measure synthesis, polarization surveys obtained by different radio telescopes, and a multiple EoR observations will help in mitigating the polarization leakages. However, further simulations and observations are necessary to pin point the best strategy for the EoR detection.

5. Future perspective

At the moment, the battle to detect the cosmological 21 cm signal is fought on two fronts. One in bettering the theoretical understanding of the Epoch of Reionization and its observational probes, while the other involves an engineering effort to develop and build next generation radio telescopes capable of detecting the cosmological 21 cm signal despite a slew of astrophysical and non-astrophysical contaminants.

The LOFAR-EoR key science project is currently in excellent shape. Almost all modules of the LOFAR-EoR end-to-end pipeline [1, 2, 4, 5, 6] are developed and the pipeline is used intensively for testing the cosmological signal extraction schemes [2, 31, 32, 33] for the extremely challenging EoR observations. The observations are carried out using WSRT radio telescope to directly measure the properties of the foreground emission in the frequency range relevant for the EoR experiments [12, 13]. On the other hand the LOFAR telescope is on schedule.

The first round of the LOFAR-EoR observations are scheduled for the end this year. Prior to those observations a shallow survey of the Northern sky will be performed. The goal of that survey is to explore the foreground emission and select the optimal LOFAR-EoR observing windows.

The near future will be very interesting and exciting. Observations with LOFAR will provide the deepest images of the low frequency radio sky. Those images, beside the primary aim of probing the EoR, can be used for additional cutting-edge scientific studies. Examples are peculiar cases of Galactic emission in total and polarized intensity, physics of the Galactic emission processes, properties the Galactic magnetic fields, distribution of the cosmic ray and thermal electrons, source counts and redshift evolution of the radio galaxies and clusters.

References

- [1] V. Jelić, *Cosmological 21cm experiments: Searching for a needle in a haystack*, PhD thesis, RuG (May, 2010) <http://dissertations.ub.rug.nl/faculties/science/2010/v.jelic/>.
- [2] V. Jelić, S. Zaroubi, P. Labropoulos, R. M. Thomas, G. Bernardi, M. A. Brentjens, A. G. de Bruyn, B. Ciardi, G. Harker, L. V. E. Koopmans, V. N. Pandey, J. Schaye, and S. Yatawatta, *Foreground simulations for the LOFAR-epoch of reionization experiment*, *MNRAS* **389** (Sept., 2008) 1319–1335, [[arXiv:0804.1130](https://arxiv.org/abs/0804.1130)].
- [3] V. Jelić, S. Zaroubi, P. Labropoulos, G. Bernardi, A. G. de Bruyn, and L. V. E. Koopmans, *Realistic Simulations of the Galactic Polarized Foreground: Consequences for 21-cm Reionization Detection Experiments*, *ArXiv e-prints* (July, 2010) [[arXiv:1007.4135](https://arxiv.org/abs/1007.4135)].
- [4] R. M. Thomas, S. Zaroubi, B. Ciardi, A. H. Pawlik, P. Labropoulos, V. Jelić, G. Bernardi, M. A. Brentjens, A. G. de Bruyn, G. J. A. Harker, L. V. E. Koopmans, G. Mellema, V. N. Pandey, J. Schaye, and S. Yatawatta, *Fast large-scale reionization simulations*, *MNRAS* **393** (Feb., 2009) 32–48, [[arXiv:0809.1326](https://arxiv.org/abs/0809.1326)].
- [5] A. R. Offringa, A. G. de Bruyn, S. Zaroubi, and M. Biehl, *A LOFAR RFI detection pipeline and its first results*, *ArXiv e-prints* (July, 2010) [[arXiv:1007.2089](https://arxiv.org/abs/1007.2089)].
- [6] P. Labropoulos, L. V. E. Koopmans, V. Jelic, S. Yatawatta, R. M. Thomas, G. Bernardi, M. Brentjens, G. de Bruyn, B. Ciardi, G. Harker, A. Offringa, V. N. Pandey, J. Schaye, and S. Zaroubi, *The LOFAR EoR Data Model: (I) Effects of Noise and Instrumental Corruptions on the 21-cm Reionization Signal-Extraction Strategy*, *ArXiv e-prints* (Jan., 2009) [[arXiv:0901.3359](https://arxiv.org/abs/0901.3359)].
- [7] P. A. Shaver, R. A. Windhorst, P. Madau, and A. G. de Bruyn, *Can the reionization epoch be detected as a global signature in the cosmic background?*, *A&A* **345** (May, 1999) 380–390, [[astro-ph/9901320](https://arxiv.org/abs/astro-ph/9901320)].
- [8] T. L. Landecker and R. Wielebinski, *The Galactic Metre Wave Radiation: A two-frequency survey between declinations $+25^\circ$ and -25° and the preparation of a map of the whole sky*, *Australian Journal of Physics Astrophysical Supplement* **16** (1970) 1–+.
- [9] S. S. Ali, S. Bharadwaj, and J. N. Chengalur, *Foregrounds for redshifted 21-cm studies of reionization: Giant Meter Wave Radio Telescope 153-MHz observations*, *MNRAS* **385** (Apr., 2008) 2166–2174, [[arXiv:0801.2424](https://arxiv.org/abs/0801.2424)].
- [10] A. E. E. Rogers and J. D. Bowman, *Spectral Index of the Diffuse Radio Background Measured from 100 TO 200 MHz*, *AJ* **136** (Aug., 2008) 641–648, [[arXiv:0806.2868](https://arxiv.org/abs/0806.2868)].
- [11] U.-L. Pen, T.-C. Chang, C. M. Hirata, J. B. Peterson, J. Roy, Y. Gupta, J. Odegova, and K. Sigurdson, *The GMRT EoR experiment: limits on polarized sky brightness at 150 MHz*, *MNRAS* (Sept., 2009) 1240–+, [[arXiv:0807.1056](https://arxiv.org/abs/0807.1056)].

- [12] G. Bernardi, A. G. de Bruyn, M. A. Brentjens, B. Ciardi, G. Harker, V. Jelić, L. V. E. Koopmans, P. Labropoulos, A. Offringa, V. N. Pandey, J. Schaye, R. M. Thomas, S. Yatawatta, and S. Zaroubi, *Foregrounds for observations of the cosmological 21 cm line. I. First Westerbork measurements of Galactic emission at 150 MHz in a low latitude field*, *A&A* **500** (June, 2009) 965–979, [[arXiv:0904.0404](#)].
- [13] G. Bernardi, A. G. d. B. G. Harker, M. A. Brentjens, B. Ciardi, V. Jelić, L. V. E. Koopmans, P. Labropoulos, A. Offringa, V. N. Pandey, J. Schaye, R. M. Thomas, S. Yatawatta, and S. Zaroubi, *Foregrounds for observations of the cosmological 21 cm line: II. Westerbork observations of the fields around 3C196 and the North Celestial Pole*, *ArXiv e-prints* (Feb., 2010) [[arXiv:1002.4177](#)].
- [14] R. A. Laing, J. M. Riley, and M. S. Longair, *Bright radio sources at 178 MHz - Flux densities, optical identifications and the cosmological evolution of powerful radio galaxies*, *MNRAS* **204** (July, 1983) 151–187.
- [15] S. E. G. Hales, J. E. Baldwin, and P. J. Warner, *The 6C survey of radio sources. II - The zone delta = 30-51 deg, alpha = 08h30m-17h30m*, *MNRAS* **234** (Oct., 1988) 919–936.
- [16] G. de Bruyn, G. Miley, R. Rengelink, and et al., *WENSS*. ASTRON, 1998.
- [17] W. Reich, *Galactic polarization surveys*, *ArXiv Astrophysics e-prints* (Mar., 2006) [[astro-ph/0603465](#)].
- [18] T. Di Matteo, R. Perna, T. Abel, and M. J. Rees, *Radio Foregrounds for the 21 Centimeter Tomography of the Neutral Intergalactic Medium at High Redshifts*, *ApJ* **564** (Jan., 2002) 576–580, [[astro-ph/0109241](#)].
- [19] T. Di Matteo, B. Ciardi, and F. Miniati, *The 21-cm emission from the reionization epoch: extended and point source foregrounds*, *MNRAS* **355** (Dec., 2004) 1053–1065, [[astro-ph/0402322](#)].
- [20] S. P. Oh and K. J. Mack, *Foregrounds for 21-cm observations of neutral gas at high redshift*, *MNRAS* **346** (Dec., 2003) 871–877, [[astro-ph/0302099](#)].
- [21] A. Cooray, *Cross-correlation studies between CMB temperature anisotropies and 21cm fluctuations*, *PhRvD* **70** (Sept., 2004) 063509+, [[astro-ph/0405528](#)].
- [22] M. G. Santos, A. Cooray, and L. Knox, *Multifrequency Analysis of 21 Centimeter Fluctuations from the Era of Reionization*, *ApJ* **625** (June, 2005) 575–587, [[astro-ph/0408515](#)].
- [23] L. Gleser, A. Nusser, and A. J. Benson, *Decontamination of cosmological 21-cm maps*, *MNRAS* **391** (Nov., 2008) 383–398, [[arXiv:0712.0497](#)].
- [24] R. J. Wilman, L. Miller, M. J. Jarvis, T. Mauch, F. Levrier, F. B. Abdalla, S. Rawlings, H. Klöckner, D. Obreschkow, D. Olteanu, and S. Young, *A semi-empirical simulation of the extragalactic radio continuum sky for next generation radio telescopes*, *MNRAS* **388** (Aug., 2008) 1335–1348, [[arXiv:0805.3413](#)].

- [25] A. de Oliveira-Costa, M. Tegmark, B. M. Gaensler, J. Jonas, T. L. Landecker, and P. Reich, *A model of diffuse Galactic radio emission from 10 MHz to 100 GHz*, *MNRAS* **388** (July, 2008) 247–260, [[arXiv:0802.1525](#)].
- [26] X. H. Sun, W. Reich, A. Waelkens, and T. A. Enßlin, *Radio observational constraints on Galactic 3D-emission models*, *A&A* **477** (Jan., 2008) 573–592, [[arXiv:0711.1572](#)].
- [27] A. Waelkens, T. Jaffe, M. Reinecke, F. S. Kitaura, and T. A. Enßlin, *Simulating polarized Galactic synchrotron emission at all frequencies. The Hammurabi code*, *A&A* **495** (Feb., 2009) 697–706, [[arXiv:0807.2262](#)].
- [28] X. H. Sun and W. Reich, *Simulated SKA maps from Galactic 3D-emission models*, *ArXiv e-prints* (Aug., 2009) [[arXiv:0908.3378](#)].
- [29] J. D. Bowman, M. F. Morales, and J. N. Hewitt, *Foreground Contamination in Interferometric Measurements of the Redshifted 21 cm Power Spectrum*, *ApJ* **695** (Apr., 2009) 183–199, [[arXiv:0807.3956](#)].
- [30] C. Jackson, *The Extragalactic Radio Sky at Faint Flux Densities*, *Publications of the Astronomical Society of Australia* **22** (2005) 36–48.
- [31] G. Harker, S. Zaroubi, G. Bernardi, M. A. Brentjens, A. G. de Bruyn, B. Ciardi, V. Jelić, L. V. E. Koopmans, P. Labropoulos, G. Mellema, A. Offringa, V. N. Pandey, J. Schaye, R. M. Thomas, and S. Yatawatta, *Non-parametric foreground subtraction for 21-cm epoch of reionization experiments*, *MNRAS* **397** (Aug., 2009) 1138–1152, [[arXiv:0903.2760](#)].
- [32] G. J. A. Harker, S. Zaroubi, R. M. Thomas, V. Jelić, P. Labropoulos, G. Mellema, I. T. Iliev, G. Bernardi, M. A. Brentjens, A. G. de Bruyn, B. Ciardi, L. V. E. Koopmans, V. N. Pandey, A. H. Pawlik, J. Schaye, and S. Yatawatta, *Detection and extraction of signals from the epoch of reionization using higher-order one-point statistics*, *MNRAS* **393** (Mar., 2009) 1449–1458, [[arXiv:0809.2428](#)].
- [33] G. Harker, S. Zaroubi, G. Bernardi, M. A. Brentjens, A. G. de Bruyn, B. Ciardi, V. Jelić, L. V. E. Koopmans, P. Labropoulos, G. Mellema, A. Offringa, V. N. Pandey, A. H. Pawlik, J. Schaye, R. M. Thomas, and S. Yatawatta, *Power spectrum extraction for redshifted 21-cm Epoch of Reionization experiments: the LOFAR case*, *MNRAS* **405** (July, 2010) 2492–2504, [[arXiv:1003.0965](#)].